Virology 409 (2011) 77–83

Contents lists available at ScienceDirect

Virology

journal homepage: www.elsevier.com/locate/yviro

Intrinsic phospholipase A2 activity of adeno-associated virus is involved in endosomal escape of incoming particles

Stefanie Stahnke [a], Kerstin Lux [b], Silke Uhrig [a,c], Florian Kreppel [d], Marianna Hösel [a,c], Oliver Coutelle [a,c], Manfred Ogris [e], Michael Hallek [a,c], Hildegard Büning [a,c,*]

[a] Department I of Internal Medicine, University of Cologne, 50924 Cologne, Germany
[b] Gene Center, University of Munich, Feodor-Lynen-Str. 25, 81377 Munich, Germany
[c] Center for Molecular Medicine Cologne, University of Cologne, Robert-Koch-Str. 21, 50931 Cologne, Germany
[d] Department of Gene Therapy, University of Ulm, Helmholtzstraße 8/1, 89081 Ulm, Germany
[e] Center for System-based Drug Research, Department of Pharmacy, Pharmaceutical Biology-Biotechnology, University of Munich, Butenandtstr. 5-13, 81377 Munich, Germany

ARTICLE INFO

Article history:
Received 8 April 2010
Returned to author for revision
12 August 2010
Accepted 22 September 2010
Available online 25 October 2010

Keywords:
phospholipase A2
AAV serotype 2
parvovirus
endosomal escape
lipolytic pore formation

ABSTRACT

The unique region of the VP1 capsid protein of adeno-associated viruses (AAV) in common with autonomously replicating parvoviruses comprises a secreted phospholipase A2 (sPLA2) homology domain. While the sPLA2 domain of Minute Virus of Mice has recently been shown to mediate endosomal escape by lipolytic pore formation, experimental evidence for a similar function in AAV infection is still lacking. Here, we explored the function of the sPLA2 domain of AAV by making use of the serotype 2 mutant ^{76}HD/AN. The sPLA2 defect in ^{76}HD/AN, which severely impairs AAV's infectivity, could be complemented *in trans* by co-infection with wild-type AAV2. Furthermore, co-infection with endosomolytically active, but not with inactive adenoviral variants partially rescued ^{76}HD/AN, providing the first evidence for a function of this domain in endosomal escape of incoming AAV particles.

Introduction

Adeno-associated viruses (AAV) are replication-defective members of the parvovirus family (Cotmore and Tattersall, 2007) that have emerged as one of the leading platforms for the development of viral vectors (Buning et al., 2008). AAV's DNA genome is packaged into a non-enveloped capsid composed of the three structural proteins VP1, VP2 and VP3 (Bleker et al., 2005). These proteins are expressed from the same open reading frame and share most of their amino acid sequence (Bleker et al., 2005). VP1 and VP2 differ from VP3 by an N-terminal extension of 65 amino acids (Bleker et al., 2005; Xie et al., 2003) whereas VP1 contains further 137 unique amino acids (Warrington et al., 2004; Xie et al., 2003). Although VP1 is dispensable for assembly and packaging of viral DNA, it is required for viral infectivity indicating the presence of functional domains within the unique VP1 region (Bleker et al., 2005; Girod et al., 2002; Kronenberg et al., 2005). Besides nuclear localization sequences found in VP1 and VP2 (Grieger et al., 2006; Sonntag et al., 2006), Zadori et al. (2001) identified a secreted phospholipase A2 (sPLA2) homology domain that is unique to VP1 and highly conserved among the parvovirus family. This domain is buried within the capsid interior but becomes externalized through pores found at the 5-fold symmetry axis during passage of AAV through the endosomal compartment (Bleker et al., 2005; Sonntag et al., 2006).

Non-parvoviral sPLA2s are known as key enzymes in lipid membrane metabolism, signal transduction pathways, inflammation, acute hypersensitivity, and degenerative diseases (Balsinde et al., 1999; Dennis, 1997; Kramer and Sharp, 1997). They hydrolyze phospholipid substrates at the 2-acyl-ester (*sn*-2) position to release lysophospholipids and free fatty acids (Zadori et al., 2001). Parvoviral sPLA2 shows the same enzymatic activity when expressed as a recombinant protein (Canaan et al., 2004). The sequence similarity of non-parvoviral and parvoviral sPLA2s is largely confined to the catalytic HDXXY domain and to the calcium binding GXG motif (Canaan et al., 2004). Mutations in either of these regions reduce the enzymatic activity and viral infectivity by several orders of magnitude, hinting at a pivotal function of the sPLA2 domain in the parvoviral life

* Corresponding author. University of Cologne, Department I of Internal Medicine and Center for Molecular Medicine Cologne (ZMMK), ZMMK Research Building, Robert-Koch-Str. 21, 50931 Cologne, Germany. Tel./fax: +49 221 478 89611/97332.
E-mail addresses: schlemms@uni-koeln.de (S. Stahnke), lux@lmb.uni-muenchen.de (K. Lux), silke.uhrig@uni-koeln.de (S. Uhrig), florian.kreppel@uni-ulm.de (F. Kreppel), marianna.hoesel@uni-koeln.de (M. Hösel), oliver.coutelle@gmail.com (O. Coutelle), Manfred.Ogris@cup.uni-muenchen.de (M. Ogris), michael.hallek@uni-koeln.de (M. Hallek), hildegard.buening@uk-koeln.de (H. Büning).

0042-6822/$ – see front matter © 2010 Elsevier Inc. All rights reserved.
doi:10.1016/j.virol.2010.09.025

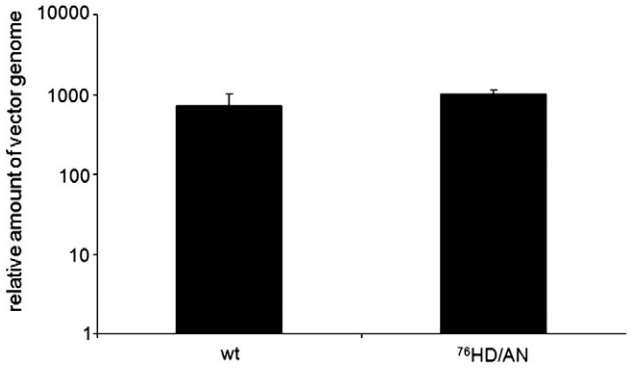

Fig. 1. Quantification of cell entry efficiency. HeLa cells were incubated with 10^4 genomic particles per cell (GOI) of rAAV2-wt (wt) or the sPLA2 mutant ^{76}HD/AN (^{76}HD/AN), respectively, for 30 min on ice followed by 1 h at 37 °C. Unbound and cell membrane bound vector particles were removed, total DNA was isolated and assayed for vector genomes by qPCR using GAPDH as a reference gene. Vector genomes encoded for the reporter gene GFP in a self-complementary vector genome conformation. Background levels obtained for untreated cells were subtracted. Values are shown as means ± SD ($n = 3$).

cycle (Girod et al., 2002; Li et al., 2001; Zadori et al., 2001). Recently, Farr et al. reported that polyethyleneimine (PEI)-induced endosomal rupture or co-infection with endosomolytically active adenoviruses partially rescued the infectivity of a catalytic center sPLA2 mutant (H42R) of the autonomously replicating parvovirus Minute Virus of Mice (MVM). They concluded that the sPLA2 activity plays a role in breaching the endosomal membrane to facilitate endosomal escape of incoming MVM particles (Farr et al., 2005).

Although AAV—as a replication-defective member of the parvovirus family—differs substantially in its virus–cell interaction from the autonomously replicating parvoviruses (Cotmore and Tattersall, 2007), it has been postulated that AAV's sPLA2 homology domain serves the same function. In order to explore this hypothesis, we compared recombinant AAV serotype 2 vectors with wild-type sPLA2 activity to our previously described sPLA2 catalytic center mutant ^{76}HD/AN (Girod et al., 2002). The sPLA2 defect in ^{76}HD/AN, which had no impact on cellular uptake, could be partially rescued by co-infection with endosomolytically active, but not with inactive adenoviral variants, leading to the conclusion that sPLA2 mutants are trapped in endosomes. These data provide the first experimental evidence for a function of sPLA2 in endosomal escape of incoming adeno-associated viruses revealing that replication-defective, i.e. helper-virus-dependent, and autonomously replicating parvoviruses use the same strategy to escape lysosomal degradation.

Results and discussion

In 2002, we reported on the cloning of four sPLA2 mutants of AAV serotype 2 (AAV2), where we had either replaced the catalytic center histidine (^{75}H) and aspartate (^{76}D) residues by alanine (A) and asparagine (N) (^{76}HD/AN) or introduced deletions into the calcium binding loop (ΔXX, ΔBH and ΔBH + L) (Girod et al., 2002). Consistent with a function of the sPLA2 homology domain in endosomal escape of incoming AAV particles, the mutants showed a delayed onset and low expression level of the Rep gene products, but no defects in capsid assembly, viral genome packaging, cell surface binding, cell entry or intracellular trafficking. However, experimental evidence for an involvement of sPLA2 in endosomal escape is still lacking. The purpose of this study was therefore to examine whether the poor infectivity of sPLA2 mutants of AAV2 could be rescued by breaking endosomal integrity. Out of the four mutants, we chose ^{76}HD/AN (Girod et al., 2002) as the closest equivalent to the MVM mutant H42R used by Farr et al. (2005). To minimize bias due to the helper virus dependency of AAV for viral gene expression, we generated ^{76}HD/AN as a recombinant vector encoding for the enhanced green fluorescent protein (GFP) in a self-complementary vector genome conformation. For comparison, the same vector genome was packaged into AAV2 capsids with a wild-type (wt) sPLA2 activity (rAAV2-wt). In line with our previous report (Girod et al., 2002), rAAV2-wt and ^{76}HD/AN were indistinguishable in terms of packaging efficiency (data not shown) and their ability to enter HeLa cells (Fig. 1) and to accumulate in the perinuclear area (Fig. 2A), but differed significantly in the amount of vector genomes available in the nucleus for gene expression as indicated by the mutant's delayed onset in transgene expression and the low transduction efficiency (Fig. 2B). The latter becomes even more obvious when a lower genomic particle per cell ratio (GOI) is used: for example at a GOI of 1000 the transduction efficiency of ^{76}HD/

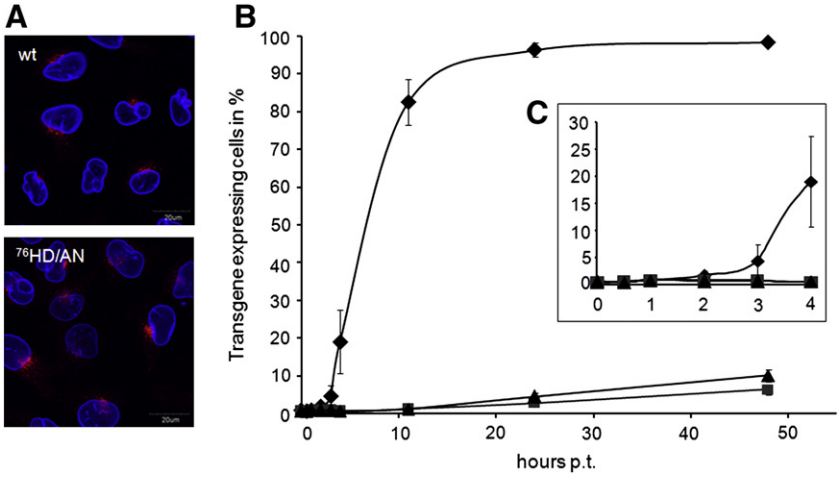

Fig. 2. Kinetic of rAAV2-wt- and ^{76}HD/AN-mediated transgene expression. A) HeLa cells were infected with rAAV2-wt (wt) or ^{76}HD/AN and fixed at 2 h p.t. Intact capsids were stained with the monoclonal anti-capsid antibody A20 (and RRX-conjugated secondary antibody), and nuclear lamina was visualized by a polycloncal anti-Lamin B IgG antibody (and Cy5-conjugated secondary antibody). B) HeLa cells were incubated with rAAV2-wt (GOI of 10^4, diamond) or ^{76}HD/AN (GOI of 10^4 (square) and 10^5 (triangle)), respectively. Both vectors encode for GFP in the self-complementary vector genome conformation. Cells were harvested at 0 min, 30 min, 1 h, 2 h, 3 h, 4 h, 11 h, 24 h and 48 h p.t., and analyzed for GFP expression by flow cytometry. Values obtained for untreated cells were subtracted. Results are the mean ± SD ($n = 3$). C) Higher resolution of graph B) for the time points 0 min, 30 min, 1 h, 2 h, 3 h and 4 h p.t.

AN did not exceed the background level ($0.7 \pm 0.6\%$; $n = 4$) compared to rAAV2-wt reaching $96.1 \pm 1.7\%$ ($n = 4$).

While the sPLA2 defect could be complemented *in trans* by addition of wild-type sPLA2 activity in case of MVM (Farr et al., 2005) this was not the case in our previous study nor in the study of Zadori et al. on porcine parvovirus (Girod et al., 2002; Zadori et al., 2001). Since, in these studies (Girod et al., 2002; Zadori et al., 2001) only one mutant-to-wild-type ratio was tested, we decided to re-evaluate the question as to whether the sPLA2 activity is required for ^{76}HD/AN transduction in *cis* or *trans*. To this end, HeLa cells were co-infected with ^{76}HD/AN encoding for GFP in a self-complementary genome conformation and wild-type AAV2 virions. Assuming that the potential helper effect of AAV2's wild-type $sPLA_2$ activity has to overcome the inhibitory effect of receptor competition, we assayed a wide range of ^{76}HD/AN-to-wild-type AAV2 ratios (between 1:0.01 and 1:100). As indicated by the increase in the number of GFP-expressing cells, co-infection with wild-type AAV2 can rescue ^{76}HD/AN's defect by *trans* complementation (Fig. 3), in line with the results for MVM. However, the window of *trans* complementation activity is narrow, since a significant increase in transduction efficiency was only observed at a mutant-to-wild-type ratio of 1:1, whereas ratios of 1:100, 1:10 or 1:0.01, had either no effect or even decreased the number of transgene expressing cells.

If the sPLA2 homology domain is involved in endosomal release, addition of endosomolytically active agents such as PEI or adenovirus should increase the infectivity of the mutant. As the base level, a transduction efficiency of approximately 10% was chosen for both, ^{76}HD/AN and rAAV2-wt, (Fig. 4). First, we assayed the chemical endosomolytic agent PEI for its ability to aid ^{76}HD/AN transduction. PEI is a positively charged polymer that, after entering cells via heparan sulfate proteoglycan (HSPG) (Payne et al., 2007), is passed along the endolysosomal pathway (Lungwitz et al., 2005) and disrupts endosomal vesicles by acting as a proton sponge (Yang and May, 2008). Because both, PEI and AAV2, bind to HSPG (Payne et al., 2007; Summerford and Samulski, 1998), receptor competition is likely to occur upon co-application of PEI and AAV2. In an effort to minimize receptor competition, PEI was added to cells 1 h after they had been transduced with rAAV2-wt or ^{76}HD/AN. Nevertheless, the transduction efficiency of both, rAAV2-wt and ^{76}HD/AN, was significantly reduced in the presence of PEI (Fig. 5A). In order to explore whether the reduced transduction efficiency was due to impaired vector uptake following addition of PEI, we determined the number of intracellular particles in HeLa cells

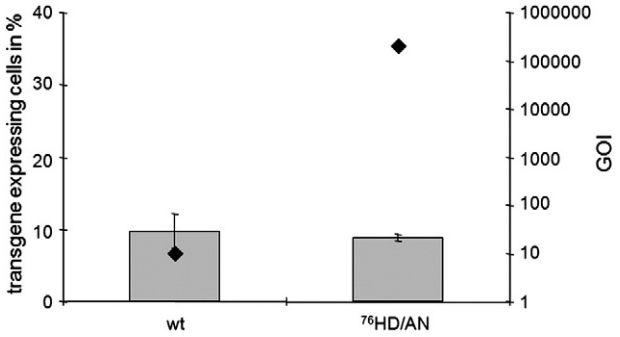

Fig. 4. Transduction efficiency of rAAV2-wt and ^{76}HD/AN. HeLa cells were incubated with a GOI of 10 of rAAV2-wt (wt) and 2×10^5 of ^{76}HD/AN, respectively, for 24 h. Cells were harvested by trypsin treatment and the percentage of transgene (GFP) expressing cells was determined by flow cytometry. Background levels obtained for untreated cells were subtracted. Results are shown as means ± SD ($n = 3$). Diamonds indicate the GOIs used for rAAV2-wt (wt) and ^{76}HD/AN, respectively.

incubated with ^{76}HD/AN for 1 and 3 h in the absence or presence of PEI (added at 1 h post transduction (p.t.)). Comparison of the values obtained at 1 h p.t. and at 3 h p.t. in the absence of PEI showed that a large proportion of vector particles entered the cells later than 1 h p.t. (Fig. 5B). Therefore, addition of PEI at 1 h p.t. likely interfered with the cellular uptake of these particles as evidenced by the reduced number of intracellular particles (Fig. 5B; gray bar vs. black bar). Hence, in contrast to MVM, PEI was not suitable to study the sPLA2 function of AAV.

Next, we investigated the effect of adenovirus on ^{76}HD/AN's transduction efficiency. Like AAV, adenovirus type 5 (Ad) is internalized by receptor-mediated endocytosis (Sanlioglu et al., 2000; Volpers and Kochanek, 2004). Upon endosomal maturation, Ad inserts an amphipatic α-helix, located at the N-terminus of structural protein VI, into the endosomal membrane leading to its dissolution (Wiethoff et al., 2005). In order to rescue ^{76}HD/AN, potentially trapped in endosomes, Ad needs to be co-localized with ^{76}HD/AN in the same endosome. Hence, we first confirmed by imaging that co-localization is possible (Fig. 6). Next, we co-infected HeLa cells with ^{76}HD/AN and an increasing concentration of wtAd (up to 500 pfu). For comparison, co-infections of rAAV2-wt and wtAd were performed. As indicated in Fig. 7A, adenovirus co-infection increased ^{76}HD/AN's transduction efficiency by up to 3.4-fold in a

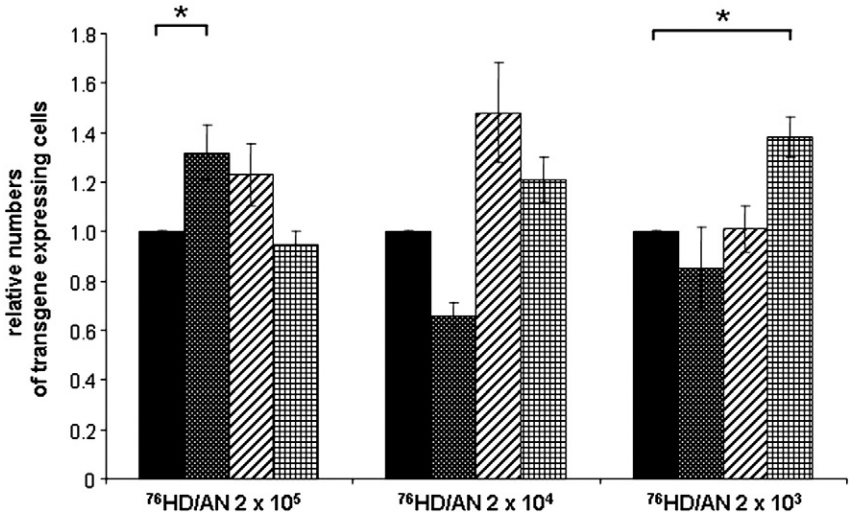

Fig. 3. Complementation assay. HeLa cells were incubated with a GOI of 2×10^5, 2×10^4 or 2×10^3, respectively, of ^{76}HD/AN encoding for GFP in the self-complementary vector genome conformation, and none (black bars), 2×10^5 (dotted bars), 2×10^4 (striped bars) or 2×10^3 (checked bars) genomic particles of wild-type AAV2 virions. Cells were harvested 24 h p.i. and analyzed for GFP expression by flow cytometry. Values obtained for untreated cells were subtracted. Results are shown as relative numbers of GFP expressing cells ± SEM ($n = 3$). *$p < 0.05$.

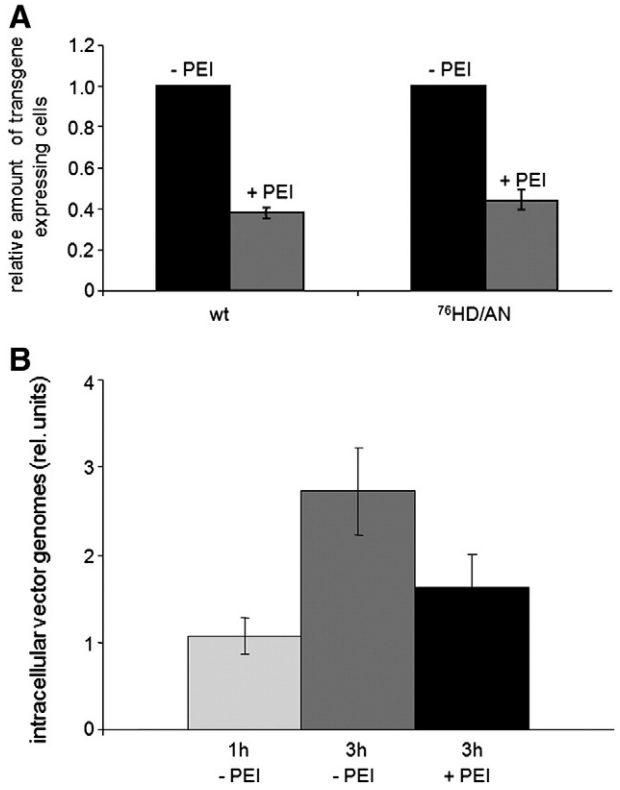

Fig. 5. Influence of PEI on the transduction efficiency. A) HeLa cells were incubated with a GOI of 10 of rAAV2-wt (wt) and a GOI of 2×10^5 of ^{76}HD/AN, respectively, in the absence (black bars) or presence (gray bars) of 40 μM branched PEI, which was added 1 h p.t. The percentage of transgene expressing cells was determined 24 h p.t. by flow cytometry. Background levels obtained for untreated cells were subtracted. Results are shown as relative numbers of GFP expressing cells ± SD ($n=3$) with values obtained in the absence of PEI set as 1. B) HeLa cells were incubated with a GOI of 500 of ^{76}HD/AN. Cells were harvested 1 h p.t. or incubated for a further 2 h in the absence (−PEI) or presence of 40 μM PEI (+PEI) at 37 °C. Total DNA was isolated and analyzed by qPCR. For normalization plasminogen activator was used as the reference gene. Results are shown as relative number of intracellular genomes ± SEM ($n=3$).

concentration-dependent manner. Although co-infection of wtAd also helped to increase the transduction efficiency of rAAV2-wt (to 2.3-fold), the helper effect on ^{76}HD/AN was significantly more pronounced (Fig. 7A).

Wild-type Ad not only possess an intrinsic endosomolytic activity (Volpers and Kochanek, 2004), but also provide helper functions for AAV2 upon adenoviral gene expression (Cotmore and Tattersall, 2007). The increased transduction efficiency of ^{76}HD/AN is thus probably due to a combination of both helper effects. To investigate this possibility, we tested the effect of high-capacity (gutless) adenoviral vectors (rAd), which are devoid of all adenoviral genes (Volpers and Kochanek, 2004) and therefore lack helper functions provided by newly produced adenoviral gene products. We co-incubated HeLa cells with increasing concentrations of rAd (up to 200 pfu) and either ^{76}HD/AN or rAAV2-wt, respectively (Fig. 7B). In contrast to wtAd, co-infection with rAd had no effect on rAAV2-wt transduction, suggesting that the increased transduction efficiency of rAAV2-wt observed in the presence of wtAd (Fig. 7A) was due to helper effects provided by adenoviral gene expression. For ^{76}HD/AN, however, an increase in transduction efficiency was observed after co-infection with rAd (Fig. 7B), consistent with a function of sPLA2 in endosomal release of the mutant. Since co-localization of both virions is required for endosomal escape, significant rescue efficiencies were only achieved at higher concentrations of rAd (Fig. 7B).

Further evidence for a function of AAV2's sPLA2 in endosomal escape was obtained by co-infection of ^{76}HD/AN and Ad2-ts1 (Gastaldelli et al., 2008), an adenoviral endosomal escape mutant (Fig. 7C). For comparison, HeLa cells were transduced with ^{76}HD/AN in the presence and absence of rAd, and with rAAV2-wt in the absence or presence of rAd and Ad2-ts1, respectively. A significant increase in the transduction efficiency of ^{76}HD/AN was seen in cells co-infected with rAd, whereas co-infection with the mutant Ad2-ts1 failed to complement the sPLA2 defect of ^{76}HD/AN (Fig. 7C). Together, these results indicate that the sPLA2 activity of AAV2 is involved in endosomal escape.

Although, like Farr et al. (2005), we made use of an sPLA2 catalytic center mutant and relied on the same helper effect, namely adenovirus-mediated endosomal disruption, the complementation

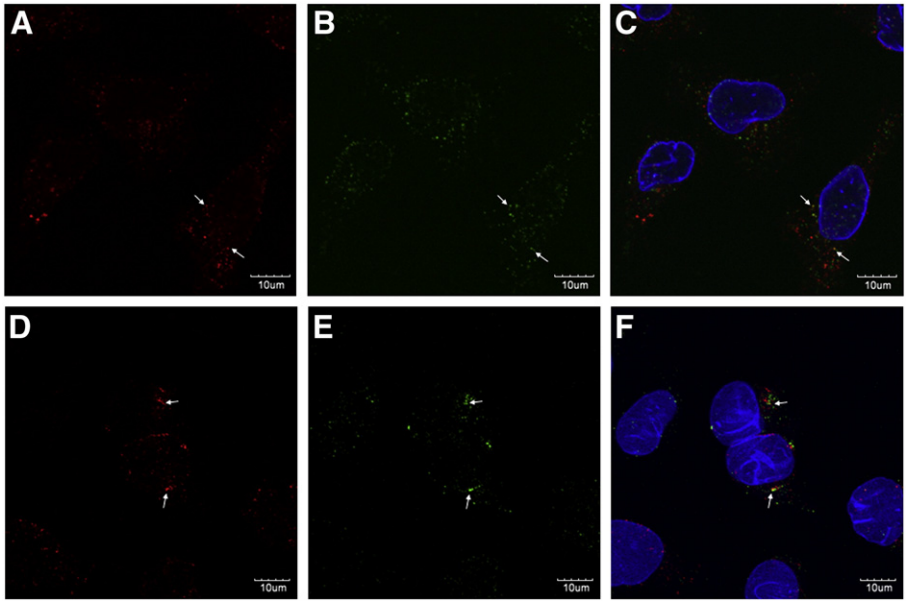

Fig. 6. Immunofluorescence staining of HeLa cells co-infected with rAAV2-wt or ^{76}HD/AN and Ad5-Alexa488. HeLa cells were infected with AAV2-wt (10^5 capsids/cell) or ^{76}HD/AN (10^5 capsids/cell) and Ad5-Alexa488 (10^4 particle/cell) for 30 min on ice, then shifted to 37 °C and incubated for further 30 min. Intact capsids were stained with the monoclonal anti-capsid antibody A20 (and RRX-conjugated secondary antibody; red), nuclear lamina was visualized by a polycloncal anti-Lamin B IgG antibody (and Cy5-conjugated secondary antibody; blue). (A) AAV2-wt capsids detected by A20. (D) ^{76}HD/AN capsids detected by A20. (B) and (E) show the Alexa488 signals of the labeled Ad5 capsids (green). (C) and (F) show the merged images of (A)/(B) and (D)/(E), respectively, and the lamina staining. Analyses were performed by confocal laser scanning microscopy.

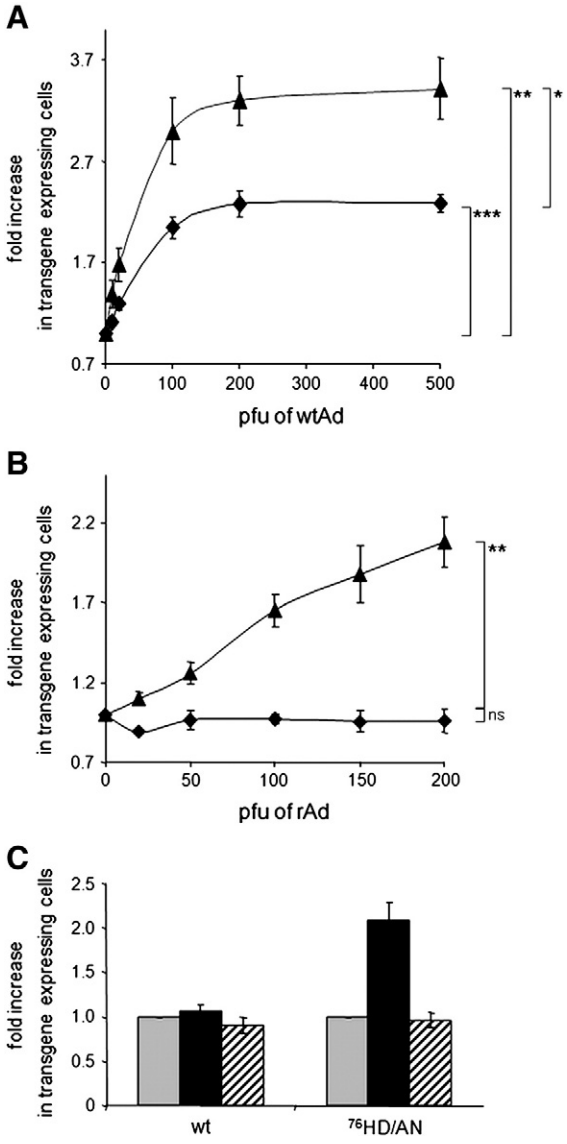

Fig. 7. Adenoviral helper effect on rAAV2-wt- and ^{76}HD/AN-mediated transductions. A) HeLa cells were infected with wtAd and ^{76}HD/AN (triangle) or rAAV2-wt (wt, diamond) for 24 h. B) HeLa cells were infected with rAd and ^{76}HD/AN (triangle) or rAAV2-wt (wt, diamond) for 24 h. C) HeLa cells were infected with rAAV2-wt (wt) or ^{76}HD/AN in the absence (gray bars) or presence of rAd (pfu of 200; black bars) or Ad2-ts1 (pfu of 200; hatched bars), respectively, for 24 h. Transduction efficiency was determined by flow cytometry. In A–C) cells were incubated with a GOI of 10 for rAAV2-wt and a GOI of 2×10^5 for ^{76}HD/AN, respectively. Background levels obtained for untreated cells were subtracted. Results are shown as fold increase in transgene expressing cells ± SEM (A, B) or SD (C) ($n=3$). *$p<0.05$; **$p<0.005$; ***$p<0.0005$; ns = not significant.

index reported for H42R clearly exceeded the rescue efficiency observed in our study. One explanation for this difference could be the simple fact that H42R was used as a replication-competent virus, while we made use of a replication-incompetent AAV vector. In the case of H42R, conceivably, incoming and newly replicated viral genomes could contribute to the production of capsids, which were used to trace viral infectivity, while in our study only the incoming vector genomes could be used as templates. Also, we cannot exclude the possibility that in A9 cells stably transduced with the Ad5 receptor CAR (Volpers and Kochanek, 2004), co-localization of Ad and H42R might occur more frequently than in the HeLa cells used in our study (Fig. 6). Furthermore, while Farr et al. carried out immunohistological analyses to determine the rescue efficiency, we employed flow cytometry.

Hence, although a direct comparison of the rescue efficiencies in both studies is difficult, the observation that adenovirus-mediated endosomal disruption resulted in a significant increase in the transduction efficiency of ^{76}HD/AN (Fig. 7) and the infectivity of H42R (Farr et al., 2005) strongly argues for sPLA2-mediated lipolytic pore formation (Mudhakir and Harashima, 2009) as an evolutionary conserved endosomal escape strategy of autonomously replicating and helper-virus-dependent members of the parvovirus family.

Material and methods

Cell culture

The human cervix epitheloid cell line HeLa (ATCC CCL-2; American Type Culture Collection, Rockville, USA) and the human embryonic kidney cell line 293 (HEK293; ATCC CRL-1573; American Type Culture Collection) were maintained as a monolayer culture at 37 °C and 5% CO_2 in Dulbecco's modified Eagle's medium (DMEM) supplemented with GlutaMax™ (Invitrogen, Darmstadt, Germany), 10% fetal calf serum, 100 U/ml penicillin and 100 mg/ml streptomycin.

Vector production and purification

AAV particles were produced in HEK293 cells by the adenovirus-free AAV production method (Hacker et al., 2005; Xiao et al., 1998). Briefly, HEK293 cells were seeded at 80% confluency and co-transfected using the calcium phosphate method with 7.5 μg of pRC (Girod et al., 1999) or pRC-HD/AN, 7.5 μg of pscAAV/EGFP (Hacker et al., 2005) and 22.5 μg of pXX6 (Xiao et al., 1998) for the production of recombinant particles or with 15 μg of plasmid of pUC-AV2 (Girod et al., 1999) or pUC-AV2-HD/AN (Girod et al., 2002) and 22.5 μg of pXX6 for production of AAV2 particles encoding for wild-type genomes without or with the HD/AN mutation, respectively. After 48 h, cells were harvested and pelleted by low-speed centrifugation. Cells were re-suspended in 150 mM NaCl/50 mM Tris–HCl (pH 8.5), freeze–thawed three times, and treated with Benzonase (50 U/ml lysate) for 30 min at 37 °C. To purify viral vector preparations, cell debris was removed by centrifugation at $3700\times g$ for 20 min at 4 °C, and the supernatant was loaded onto a discontinuous iodixanol gradient (Hacker et al., 2005). The 40% phase of the gradient, containing the vector particles, was harvested. Genomic particle titers of vector preparations were determined by quantitative (q) PCR (Theiss et al., 2003) using GFP primers (see below) or cap primers (3201, GGTACGACGACGATTGCC; 4066, ATGTCCGTCCGTGTGTGG), respectively. Capsid titers were determined by enzyme-linked immunosorbent assay (ELISA) using the anti-capsid antibody A20 (Girod et al., 1999). Monoclonal A20 hybridoma supernatant was kindly provided by Jürgen Kleinschmidt (DKFZ, Heidelberg, Germany).

Quantification of AAV entry efficiency

A total of 4×10^4 HeLa cells were seeded per well in a 12-well plate. HeLa cells were incubated with 1×10^4 genomic particles per cell of rAAV2-wt or ^{76}HD/AN, respectively. Both vectors contain the enhanced green fluorescent protein (GFP) as reporter gene under the control of the Cytomegalovirus (CMV) promoter in the self-complementary vector genome conformation. Cells were incubated on ice for 30 min, then shifted to 37 °C and incubated at 37 °C and 5% CO_2 for 1 h. Supernatant was removed and cells were washed twice with 1× PBS. Cells were harvested by trypsin treatment, pelleted, washed three times in 1× PBS, and total DNA was isolated (DNeasy Tissue Kit, Qiagen, Hilden, Germany). Relative quantification of vector genomes and reference gene (glyceraldehydes-3-phosphate

dehydrogenase (GAPDH)) was performed by qPCR using the LightCycler (LC) rapid thermal cycler system (Roche Diagnostics, Mannheim, Germany) and the SYBR Green kit (Roche Diagnostics). The following primers were chosen for vector genome and reference gene amplification: GFP_rev, 5′-CTCGATGTTGTGGCGGAT-3′ and GFP_fwd, 5′-GCGCCGAGGTGAAGTT-3′, GAPDH_fwd, 5′-GAGTCCACTGGCGTCTTCA-3′ and GAPDH_rev, 5′-TTCAGCTCAGGATGACCTT-3′. PCR amplification was performed as follows: 5 min denaturation at 95 °C, followed by 40 cycles of 15 s at 95 °C, 10 s at 60 °C, and 30 s at 72 °C. The specificity of target and reference gene amplification was confirmed by melting curve analysis. GFP values were normalized to GAPDH levels using the RelQuant software (Roche Diagnostics).

Transduction experiments

A total of 4×10^4 HeLa cells were seeded per well in a 12-well plate. After 24 h, cells were transduced by vectors as indicated. For experiments shown in Fig. 3 cells were co-infected with wild-type AAV2, for experiments in Fig. 7 co-infection was performed with adenovirus type 5, gutless recombinant adenoviral vectors type 5 or the adenoviral type 2 ts-1 mutant, respectively. Cells were incubated at 37 °C and 5% CO_2. In case of the rAAV expression kinetic, the transduction was carried out on ice for 30 min before shifted to 37 °C. If not stated otherwise, cells were harvested 24 h post transduction by trypsin treatment, re-suspended in 1× PBS, and analyzed by flow cytometry using the BD FACS Calibur system (Becton Dickinson, Heidelberg, Germany). A minimum of 10,000 cells was analyzed per sample. Data were analyzed using WinMDI 2.8 fluorescence-activated cell sorting software.

Imaging studies

A total of 4×10^4 HeLa cells per well were seeded onto 12-mm coverslips in 24-well plates. For experiment shown in Fig. 2A, HeLa cells were incubated with 10^4 genomic particles of rAAV2-wt or ^{76}HD/AN for 30 min on ice, then shifted to 37 °C and further incubated for 2 h at 37 °C and 5% CO_2. Cells were washed with 1× PBS, fixed for 15 min in 3% paraformaldehyde (PFA)/PBS at room temperature, and washed with 50 mM NH_4Cl in 1× PBS. The remaining PFA was quenched for 30 min with 50 mM NH_4Cl in 1× PBS. For antibody staining, cells were permeabilized with 0.2% Triton X-100 in 1× PBS for 10 min, blocked for 10 min with 0.2% gelatine in 1× PBS, and incubated for 1 h at room temperature with the polyclonal goat anti-Lamin B IgG antibody (1:50 in 1× PBS; Santa Cruz Biotechnology) and supernatants of monoclonal A20 mouse hybridoma cells (kindly provided by Jürgen Kleinschmidt, DKFZ). After washing and blocking, the cells were incubated for 1 h with the following secondary antibodies: Cy5-conjugated donkey anti-goat antibody (Dianova, diluted 1:100 in 1× PBS), Rhodamine Red-X (RRX)-conjugated donkey anti-mouse (Dianova, diluted 1:100 in 1× PBS). The coverslips were again washed in 1× PBS, embedded in Vectashield mounting medium (Alexis), and subjected to confocal laser scanning microscopy. For experiments shown in Fig. 6, HeLa cells were incubated with 10^5 capsids per cell of AAV2-wt (encoding for wild-type genomes) or ^{76}HD/AN (encoding for wild-type genomes with the HD/AN mutation) and Ad5-Alex488 (10^4 particle/cell, labeled with a 20-fold molar excess of amine-reactive TFP-Alexa488 (Invitrogen) over capsid surface amine groups according to Espenlaub et al., 2010) for 30 min on ice, then shifted to 37 °C and further incubated at 37 °C and 5% CO_2 for 30 min. All subsequent steps were conducted as described above. For nuclear staining, polyclonal goat anti-lamin B IgG antibody (1:50 in 1× PBS; Santa Cruz Biotechnology) and for detection of AAV capsids supernatants of monoclonal A20 mouse hybridoma cells (kindly provided by Jürgen Kleinschmidt, DKFZ) was used. As secondary antibodies Cy5-conjugated donkey anti-goat antibody (Dianova, diluted 1:100 in 1× PBS) and Rhodamine Red-X (RRX)-conjugated donkey anti-mouse (Dianova, diluted 1:100 in 1× PBS) were applied.

Chemically induced endosomolysis

For FACS analysis, a total of 4×10^4 HeLa cells were seeded per well in a 12-well plate. After 24 h, HeLa cells were incubated with a GOI of 10 of rAAV2-wt and 2×10^5 of ^{76}HD/AN, respectively, for 30 min on ice and followed by 1 h at 37 °C. Branched PEI (average molecular weight 25 kDa (Sigma-Aldrich, Munich, Germany); 1 mg/ml stock solution neutralized with hydrochloric acid to pH 7.1) was added to the medium at a final concentration of 40 μM and cells were analyzed 23 h post PEI addition by flow cytometry. For qPCR analysis, a total of 4×10^4 HeLa cells were seeded per well in a 12-well plate. After 24 h, HeLa cells were incubated with a GOI of 500 of ^{76}HD/AN for 30 min on ice followed by 1 h incubation at 37 °C. The "1 h samples" were harvested by trypsin treatment and total DNA was isolated (DNeasy Tissue Kit, Qiagen). Furthermore, cells were incubated for further 2 h at 37 °C in the absence or presence of 40 μM PEI. Subsequently, cells were harvested and DNA was isolated as described above. Relative quantification of vector genomes and reference gene was performed by qPCR as described above using GFP (see above) and plasminogen activator (PLAT) primers (PLAT_fw, ACCTAGACTGGATTCGTG, PLAT_rev, AGAGGCTAGTGTGCAT), respectively. The specificity of target and reference gene amplification was confirmed by melting curve analysis. Values obtained for the target gene were normalized to PLAT levels using the RelQuant software (Roche Diagnostics).

Statistical analysis

Statistical analyses were performed using the Student's *t*-test. A value of $P<0.05$ was considered as statistically significant.

Acknowledgment

This work was supported by Deutsche Forschungsgemeinschaft (SFB 670 [H.B. and M.H.] and SPP1230 [H.B., M.H., M.O. and F.K.]) and the Center for Molecular Medicine Cologne (ZMMK) [H.B. and M.H.]. Furthermore, we thank Richard Jude Samulski (University of North Carolina at Chapel Hill, USA) and Jürgen Kleinschmidt (DKFZ) for kindly providing pXX6 and the anti-capsid antibody A20, respectively, and Urs Greber (University of Zurich, Zurich, Switzerland) for providing Ad2-ts1.

References

Balsinde, J., Balboa, M.A., Insel, P.A., Dennis, E.A., 1999. Regulation and inhibition of phospholipase A2. Annu. Rev. Pharmacol. Toxicol. 39, 175–189.

Bleker, S., Sonntag, F., Kleinschmidt, J.A., 2005. Mutational analysis of narrow pores at the fivefold symmetry axes of adeno-associated virus type 2 capsids reveals a dual role in genome packaging and activation of phospholipase A2 activity. J. Virol. 79 (4), 2528–2540.

Buning, H., Perabo, L., Coutelle, O., Quadt-Humme, S., Hallek, M., 2008. Recent developments in adeno-associated virus vector technology. J. Gene Med. 10 (7), 717–733.

Canaan, S., Zadori, Z., Ghomashchi, F., Bollinger, J., Sadilek, M., Moreau, M.E., Tijssen, P., Gelb, M.H., 2004. Interfacial enzymology of parvovirus phospholipases A2. J. Biol. Chem. 279 (15), 14502–14508.

Cotmore, S.F., Tattersall, P., 2007. Parvoviral host range and cell entry mechanisms. Adv. Virus Res. 70, 183–232.

Dennis, E.A., 1997. The growing phospholipase A2 superfamily of signal transduction enzymes. Trends Biochem. Sci. 22 (1), 1–2.

Espenlaub, S., Corjon, S., Engler, T., Fella, C., Ogris, M., Wagner, E., Kochanek, S., Kreppel, F., 2010. Capsomere-specific fluorescent labeling of adenovirus vector particles allows for detailed analysis of intracellular particle trafficking and of the performance of bioresponsive bonds for vector capsid modifications. Hum. Gene Ther. 21 (9), 1155–1167.

Farr, G.A., Zhang, L.G., Tattersall, P., 2005. Parvoviral virions deploy a capsid-tethered lipolytic enzyme to breach the endosomal membrane during cell entry. Proc. Natl. Acad. Sci. USA 102 (47), 17148–17153.

Gastaldelli, M., Imelli, N., Boucke, K., Amstutz, B., Meier, O., Greber, U.F., 2008. Infectious adenovirus type 2 transport through early but not late endosomes. Traffic 9 (12), 2265–2278.
Girod, A., Ried, M., Wobus, C., Lahm, H., Leike, K., Kleinschmidt, J., Deleage, G., Hallek, M., 1999. Genetic capsid modifications allow efficient re-targeting of adeno-associated virus type 2. Nat. Med. 5 (9), 1052–1056.
Girod, A., Wobus, C.E., Zadori, Z., Ried, M., Leike, K., Tijssen, P., Kleinschmidt, J.A., Hallek, M., 2002. The VP1 capsid protein of adeno-associated virus type 2 is carrying a phospholipase A2 domain required for virus infectivity. J. Gen. Virol. 83 (Pt 5), 973–978.
Grieger, J.C., Snowdy, S., Samulski, R.J., 2006. Separate basic region motifs within the adeno-associated virus capsid proteins are essential for infectivity and assembly. J. Virol. 80 (11), 5199–5210.
Hacker, U.T., Wingenfeld, L., Kofler, D.M., Schuhmann, N.K., Lutz, S., Herold, T., King, S.B., Gerner, F.M., Perabo, L., Rabinowitz, J., McCarty, D.M., Samulski, R.J., Hallek, M., Buning, H., 2005. Adeno-associated virus serotypes 1 to 5 mediated tumor cell directed gene transfer and improvement of transduction efficiency. J. Gene Med. 7 (11), 1429–1438.
Kramer, R.M., Sharp, J.D., 1997. Structure, function and regulation of Ca2+-sensitive cytosolic phospholipase A2 (cPLA2). FEBS Lett. 410 (1), 49–53.
Kronenberg, S., Bottcher, B., von der Lieth, C.W., Bleker, S., Kleinschmidt, J.A., 2005. A conformational change in the adeno-associated virus type 2 capsid leads to the exposure of hidden VP1 N termini. J. Virol. 79 (9), 5296–5303.
Li, Y., Zadori, Z., Bando, H., Dubuc, R., Fediere, G., Szelei, J., Tijssen, P., 2001. Genome organization of the densovirus from Bombyx mori (BmDNV-1) and enzyme activity of its capsid. J. Gen. Virol. 82 (Pt 11), 2821–2825.
Lungwitz, U., Breunig, M., Blunk, T., Gopferich, A., 2005. Polyethylenimine-based non-viral gene delivery systems. Eur. J. Pharm. Biopharm. 60 (2), 247–266.
Mudhakir, D., Harashima, H., 2009. Learning from the viral journey: how to enter cells and how to overcome intracellular barriers to reach the nucleus. AAPS J. 11 (1), 65–77.
Payne, C.K., Jones, S.A., Chen, C., Zhuang, X., 2007. Internalization and trafficking of cell surface proteoglycans and proteoglycan-binding ligands. Traffic 8 (4), 389–401.
Sanlioglu, S., Benson, P.K., Yang, J., Atkinson, E.M., Reynolds, T., Engelhardt, J.F., 2000. Endocytosis and nuclear trafficking of adeno-associated virus type 2 are controlled by rac1 and phosphatidylinositol-3 kinase activation. J. Virol. 74 (19), 9184–9196.
Sonntag, F., Bleker, S., Leuchs, B., Fischer, R., Kleinschmidt, J.A., 2006. Adeno-associated virus type 2 capsids with externalized VP1/VP2 trafficking domains are generated prior to passage through the cytoplasm and are maintained until uncoating occurs in the nucleus. J. Virol. 80 (22), 11040–11054.
Summerford, C., Samulski, R.J., 1998. Membrane-associated heparan sulfate proteoglycan is a receptor for adeno-associated virus type 2 virions. J. Virol. 72 (2), 1438–1445.
Theiss, H.D., Kofler, D.M., Buning, H., Aldenhoff, A.L., Kaess, B., Decker, T., Baumert, J., Hallek, M., Wendtner, C.M., 2003. Enhancement of gene transfer with recombinant adeno-associated virus (rAAV) vectors into primary B-cell chronic lymphocytic leukemia cells by CpG-oligodeoxynucleotides. Exp. Hematol. 31 (12), 1223–1229.
Volpers, C., Kochanek, S., 2004. Adenoviral vectors for gene transfer and therapy. J. Gene Med. 6 (Suppl 1), S164–S171.
Warrington Jr., K.H., Gorbatyuk, O.S., Harrison, J.K., Opie, S.R., Zolotukhin, S., Muzyczka, N., 2004. Adeno-associated virus type 2 VP2 capsid protein is nonessential and can tolerate large peptide insertions at its N terminus. J. Virol. 78 (12), 6595–6609.
Wiethoff, C.M., Wodrich, H., Gerace, L., Nemerow, G.R., 2005. Adenovirus protein VI mediates membrane disruption following capsid disassembly. J. Virol. 79 (4), 1992–2000.
Xiao, X., Li, J., Samulski, R.J., 1998. Production of high-titer recombinant adeno-associated virus vectors in the absence of helper adenovirus. J. Virol. 72 (3), 2224–2232.
Xie, Q., Somasundaram, T., Bhatia, S., Bu, W., Chapman, M.S., 2003. Structure determination of adeno-associated virus 2: three complete virus particles per asymmetric unit. Acta Crystallogr. D Biol. Crystallogr. 59 (Pt 6), 959–970.
Yang, S., May, S., 2008. Release of cationic polymer-DNA complexes from the endosome: a theoretical investigation of the proton sponge hypothesis. J. Chem. Phys. 129 (18), 185105.
Zadori, Z., Szelei, J., Lacoste, M.C., Li, Y., Gariepy, S., Raymond, P., Allaire, M., Nabi, I.R., Tijssen, P., 2001. A viral phospholipase A2 is required for parvovirus infectivity. Dev. Cell 1 (2), 291–302.